# Defining an Electrophysiological Phenotype and Increasing Survival in Amyotrophic Lateral Sclerosis Patient-Derived Motor Neurons

# Table of Contents

## Glossary of abbreviations

| | |
|---|---|
| AAV1 | Adeno-Associated Virus 1 |
| ALS | Amyotrophic Lateral Sclerosis |
| ANOVA | Analysis of Variance |
| ER | Endoplasmic Reticulum |
| FACS | Fluorescence-Activated Cell Sorting |
| FUS | Fused-in-Sarcoma |
| GFP | Green Fluorescent Protein |
| iPSC | Induced Pluripotent Stem Cells |
| MEA | Microelectrode Arrays |
| SEM | Standard Error of the Mean |
| *SOD1* | Cu-Zn Superoxide Dismutase 1 |
| RFP | Red Fluorescent Protein |

## Section 1: Introduction

Amyotrophic Lateral Sclerosis - or Lou Gherig's disease, as it is known in the United States in honor of the great baseball player who developed the disease in the 1930s - is a rapidly progressive, currently untreatable, and highly fatal neurodegenerative disease of the human motor nervous system involving both lower and upper motor neurons[1]. Descriptions of ALS cases have been found in the medical literature as early as 1824, but it was in the late 19th century that the famous French physician and neurobiologist Jean-Martin Charcot first reported on the relationship between the clinical signs of the disease and its associated autopsy findings[3]. Prevalence rates in Europe and North America have ranged between 2.7 to 7.4 people per 100,000 persons, with an incidence between 1.5 to 2.7 per 100,000 persons/year[4,5]. ALS usually manifests in mid-life, with most cases diagnosed between the ages of 50 and 60[6], although its incidence increases with every decade after 40 years old and peaks at age 74[4].
The cause is unknown in a majority of cases of ALS, with 90 to 95 percent of patients presenting with sporadic forms of the disease, while only 5 to 10 percent suffering forms with a clear familial inheritance[6]. Several genes have been identified as causal in the familial form - as well as a minority of sporadic cases. The most commonly involved gene is *C9orf72* - so called as a reference to the usual position of the "open reading frame" in chromosome nine -, which is responsible for 40 to 50 percent of cases of familial ALS as well as 10 percent of sporadic cases[7]. The exact pathogenic mechanism by which the *C9orf72* gene mutation leads to the disease remains unclear, but some proposed pathways include loss of function; toxicity conferred by RNA sequences derived from *C9orf72* genes containing an abnormally high number of the hexanucleotide GGGGCC repeats (normally <30 but as high as 700-1600 in affected patients)[8]; and toxicity conferred by the creation of dipeptide repeat proteins.
The second most commonly involved gene is the Cu-Zn superoxide dismutase 1 (*SOD1*) gene, which accounts for around 20 to 25 percent of hereditary cases[2], along with 1 to 2 percent of sporadic cases[6]. Similar to *C9orf72*, the exact pathogenic effects of the *SOD1* mutation remain unclear, but pathways proposed include aberrant redox activity and abnormal aggregation of mutant *SOD1* protein in motor neurons[2]. What does appear clear is that the pathogenesis of the *SOD1* gene mutation is not related to loss of function, as animal experiments involving deletion of the gene do not lead to the manifestation of the disease. Another gene identified as causal in ALS is the fused-in-sarcoma gene (*FUS*), which gives rise to an RNA binding protein that may become mislocalized to the cytoplasm in mutant forms leading to its abnormal aggregation.

Several hypotheses exist to explain the relationship between the aforementioned genetic mutations -as well as others - and the clinical and pathologic manifestations of the disease, namely the observed early cell death of upper and lower motor neurons. The four leading hypotheses include: 1) oxidative damage (prompted by the discovery of the *SOD1* mutation), 2) axonal dysfunction from neurofilamentous disorganization (supported by the finding of abnormal accumulation of neurofilaments as a pathological feature of many cases of sporadic and *SOD1*-mediated familial disease), 3) toxicity from intracellular aggregates and/or failure of protein folding or degradation (common in *SOD1*- and *FUS*-associated cases), and 4) excitotoxic death[6].

It was the latter hypothesis that we were interested in exploring. Under the excitotoxicity theory, some have posited that problems in the appropriate retrieval of the neurotransmitter glutamate from the synaptic cleft by astrocytes lead to increased post-synaptic motor neuron stimulation, increased levels of intracellular calcium, and eventually cell death[6]. Support for this theory arose from the discovery of large increases in the levels of glutamate in the cerebrospinal fluid of ALS patients and reduced astrocytic glutamate transport. What is particularly interesting is the fact that these abnormally increased levels are observed not only in familial cases, but also in up to 40 percent of sporadic cases. Nevertheless, nerve conduction studies evaluating axonal threshold (strength-duration time constant and recovery cycle times) in ALS patients have demonstrated increased axonal membrane excitability well away from any synapses[9–12], and the degree of hyperactivity correlates with patient survival[10]. These findings bring the causal relationship between glutamate and excitotoxicity into question, and instead raise the possibility of intrinsic causes existing to explain this observed motor neuron hyperactivity.

Studies of ALS have so far been limited by the availability of mouse models and/or viable cell lines[6]. Transgenic mice that overexpress the G93A mutation of the human *SOD1* gene (h*SOD1*(G93A) mice) are one of the most commonly used and accepted animals models[13]. Studies using h*SOD1*(G93A) mice have indeed confirmed higher levels of baseline activity of diseased motor neurons, and have identified increased persistent sodium currents as causal, at least partly[14]. However, it remains unknown whether this increased neural activity is a common feature shared by other genetic causes of ALS such as those caused by *C9orf72* or *FUS* mutations, and this is mainly due to the lack of availability of representative mouse models.

The ability to derive motor neurons from human iPSCs obtained from both ALS patients as well as healthy controls has greatly facilitated the study of the electrophysiological properties of ALS neurons, as well as several other neurodegenerative disorders. As presented by Takahashi et al. in their

publication in 2007, iPSCs derived from human dermal fibroblasts treated with four transcription factors (OCT 3/4, SOX2, KLF4, and c-Myc) are similar to human embryonic stem cells in morphology, proliferation, surface antigens, gene expression, epigenetic status of pluripotent cell-specific genes, and telomerase activity[15]. Further advancements introduced by Dimos et al. in their publication in 2008, allowed for the differentiation of patient-derived iPSCs into ALS motor neurons and glia[16]. This technology has permitted for the generation of patient-specific ALS motor neurons, representing several disease-causing mutations. Though motor neurons obtained from patient and control-derived iPSCs have already been used to study the pathogenic mechanisms of ALS, these studies have so far been limited by a small number of cell lines, thus proving difficult to generalize across other cell lines and patients[17]. We overcame this limitation in this study by deriving cell lines from eight different ALS patients bearing three different ALS-causing mutations (*SOD1* mutation, *C9orf72* repeat expansions, and *FUS* mutation) and compared them to motor neurons derived from iPSCs originating from five healthy controls. We further used gene-targeted correction of the disease-causing *SOD1* mutation to produce otherwise isogenic stem cells bearing wild-type *SOD1* alleles[18]. This constituted the largest sample of ALS motor neurons studied to date. We began our exploration by characterizing the intrinsic neuronal activity of ALS motor neurons in comparison to controls utilizing MEA technology -which allows for the simultaneous detection of single-unit activity within a large population of cultured cells by a 64-electrode array embedded directly within the culture well- and correlated it to cell life span for both ALS and control neurons. We then used whole-cell patch-clamp technology to explore the specific behavior of the different ion channels that control/affect neuronal firing, and determined that ALS-derived motor neurons have reduced delayed-rectifier voltage-gated potassium currents in comparison to controls. In all experiments, we ensured the blockade of both excitatory and inhibitory neurotransmitters in order to examine only the intrinsic properties of these neurons. We then reversed a disease-causing mutation using zinc fingers-based genetic targeting and ensured cell hyperactivity as well as cell life returned to baseline. Most importantly, we utilized the drug retigabine -a known activator of Kv7 delayed-rectifier potassium channels, and an FDA-approved drug for the treatment of epilepsy- to increase delayed-rectifier potassium currents in order to reverse the previously measured cell hyperactivity, which led to an improvement in cell survival.

The aforementioned reduction in hyperexcitability held true across all cell lines originating from patients with *SOD1*, *C9orf72*, and *FUS* mutations, thus raising the possibility of evaluating retigabine in a safety study in humans.

The work presented in this report has been previously published in the journal *Cell Reports,* on April 3, 2014, as an article titled "Intrinsic Membrane Hyperexcitability of Amyotrophic Lateral Sclerosis Patient-Derived Motor Neurons", primary authored by Brian Wainger, M.D., PhD et al.[19]

Numa Perez, the author of this Scholarly Project Report, was a co-author of the aforementioned scientific journal article, and was directly responsible for conducting the experiments using MEAs, as well as analyzing the resulting data, to include writing all MATLAB code necessary to accomplish this task. His work directly resulted in Figures 1B-G, 3D, 4, and 5A of this report, with corresponding figures in the original journal article.

All generation and molecular analysis of iPSC-derived motor neurons was conducted by members of the laboratory of Kevin Eggan, PhD, at the Harvard Department of Stem Cell & Regenerative Biology. All patch-clamp experiments were conducted by Cassidy Mellin and Brian Wainger, M.D., PhD, members at the time of the laboratory of Clifford Woolf, MB, BCh, PhD, at the FM Kirby Neurology Center, Boston Children's Hospital. All statistical analysis was conducted by Brian Wainger, M.D. with the assistance of K. Kapur. All figures were modified from MATLAB originals and/or directly created by Brian Wainger, M.D., PhD, with the assistance of K. Wainger.

# Section 2: Methods

## iPSC Lines, Culture, and Motor Neuron Differentiation

iPSC generation from patient fibroblasts obtained under institutional review board approval, characterization, and motor neuron differentiation were performed as described in Kiskinis et al. (2014), with iPSC line scoring as done previously[20]. For transfection of 18a and 39b lines with an Hb9::GFP reporter, a 1 kb Hb9 promoter fragment (gift from Hynek Wichterle) controlling the expression of myristoylated GFP was inserted into a donor plasmid specific for the AAVS1 locus (Sigma). Subsequently, 2.5 million iPSCs were accutased and electroporated using the Neon transfection system (100 µl tip; 1,600 V voltage, 20 ms width, 1 pulse; Life Technologies) with 2 µg of AAVS1 ZFN plasmid and 6 µg of modified AAVS1 donor plasmid. After nucleofection, cells were plated on matrigel with mTeSR1 in the presence of ROCK inhibitor. After 48 hr, puromycin selection was applied, and surviving clonal colonies were individually passaged and genomic DNA was extracted. PCR was used to confirm proper targeting of the cassette. Primer sequences are available upon request. Faithful expression of the reporter was verified using expression of the motor neuron marker Isl1.

iPSCs were maintained on culture dishes as described previously[21] with modifications [18] in a 24 day protocol based on initial neuralization with SB431542 (10 µM, Sigma-Aldrich) and Dorsomorphin (1 µM, Stemgent), and motor neuron patterning with RA (Sigma) and a small smoothened Agonist 1.3 (Calbiochem). FACS-purified neurons were grown on a confluent monolayer of primary cortical mouse glia prepared from P0–P2 mouse pups (as described in Boulting et al., 2011), which may increase firing rates compared to experiments without glia[22]).

## MEA Recording

After 24 days of differentiation, equal numbers of control and ALS neurons were plated on poly-D-lysine/laminin coated p515A probes (Alpha Med Scientific) or M768-GLx 12-well plates (Axion BioSystems) at typical densities of 40,000 to 80,000 cells/probe or well. All probes were visualized immediately before each recording session to confirm a full monolayer of cells. Initial experiments (11a, 18a, 39b, and RB9d comparison) were performed as close as possible to the time of patch recordings (4 weeks). However, because we wished to evaluate firing at a time point prior to significant motor neuron death[18], we performed subsequent experiments (39b-Cor and 39b comparison and all later experiments) at day 14 after dissociation.

Recordings from 64 extracellular electrodes were made using a Med64 (Alpha Med Scientific) or Maestro (Axion BioSystems) MEA recording amplifier with a head stage that maintained a temperature of 37°C. For Med64 recordings, data were sampled at 20 kHz, digitized, and analyzed by spike clustering and spike extraction algorithms using Mobius software (Alpha Med Scientific) with a 2 kHz 9-pole Bessel low pass filter, 10 µV action threshold detection limit, and 30% cluster similarity radius. These standard settings were maintained for all analyses. We confirmed that we obtained similar results across a wide range of action potential threshold and cluster similarity radius settings. Correlation analysis to detect and correct for clusters detected by multiple electrodes was performed using custom MATLAB software. Total action potential firing rates and mean neuronal firing frequencies were then determined and plotted. In order to record in larger replicates, we used the Axion Maestro MEA device, in a 12-well format with 64 extracellular electrodes in each well. For Maestro recordings, data were sampled at 12.5 kHz, digitized, and analyzed using Axion Integrated Studio software (Axion BioSystems) with a 200 Hz high pass and 2.5 kHz low pass filter and an adaptive spike detection threshold set at 5.5 times the SD

for each electrode with 1 sec binning. These standard settings were maintained for all Axion MEA recording and analysis.

For retigabine dose-response curves, action potential numbers during 1 min of recording in each concentration of retigabine were normalized to the initial action potential number during 1 min of recording in standard extracellular saline solution. The $EC_{50}$ value was determined by fitting the mean normalized data values to the Hill equation, $y = 1/((EC_{50}/x)^{nH}+1)$ where nH is the Hill coefficient.

## Patch Electrophysiology

Whole-cell patch recordings were performed on iPSC-derived motor neurons identified by transduction with an Hb9::RFP lentivirus. Lentiviral transduction was typically performed 7 to 10 days before recording. Two large comparisons were performed, one consisting of 11a, 18a, 39b, and RB9d, and the second consisting of 39b-Cor and 39b. Each comparison was made from pooled data from multiple separate experiments, each consisting of synchronous and parallel iPSC culture and differentiation, embryoid body dissociation, plating, and maturation of control- and ALS-derived neurons. Equal numbers of control and ALS motor neurons were recorded from each experiment. Comparison of the original four lines (11a, 18a, 39b, and RB9d) was made using four separate parallel differentiation experiments, whereas comparison of the isogenic correction comparison (39b-Cor and 39b) was performed using three separate parallel differentiation experiments.

For each experiment, neurons from control and ALS lines were dissociated after 24 days of differentiation and plated onto poly-d-lysine/laminin coated glass coverslips (20,000 to 40,000 cells/coverslip) and allowed to mature for four weeks from start of differentiation. We chose four weeks as the best time point because this yielded the most homogeneous population of mature-appearing Hb9::RFP-positive motor neurons (at the requisite low cell density for patch clamp) with the most mature electrophysiological properties. Whole-cell current-clamp and voltage-clamp recordings were performed using a Multiclamp 700B (Molecular Devices) at room temperature (21°C–23°C). Data were sampled at 20 kHz and digitized with a Digidata 1440A A/D interface and recorded using pCLAMP 10 software (Molecular Devices). Data were low-pass filtered at 2 kHz. Patch pipettes were pulled from borosilicate glass capillaries on a Sutter Instruments P-97 puller and had resistances of 2–4 MΩ. The pipette capacitance was reduced by wrapping the shank with Parafilm and compensated for using the

amplifier circuitry. Series resistance was typically 5–10 MΩ, always less than 15 MΩ, and compensated by at least 80%. Neurons were excluded from analysis if holding current at −80 mV exceeded 100 pA, input resistance was less than 250 or greater than 2000 MΩ, or spikes elicited from −65 mV had peaks below 0 mV. Resting membrane potential was determined by averaging for 20 s of recording, and afterward a small holding current (typically with amplitude less than 5 pA) was used to clamp the resting membrane potential as close as possible to −65 mV. Rheobase was measured by applying 1 sec steps in increments of 2.5 pA until an action potential was generated. Current ramps were elicited from an initial hyperpolarizing current of 10 pA for 1 sec followed by a 210 pA/sec depolarizing ramp of duration 1 sec. Spikes on the ramps were counted if the peak voltage exceeded −10 mV. Action potential properties were determined using custom-written analysis software in Igor Pro (Wavemetrics) with DataAccess (Bruxton) for importing the files. For voltage-clamp recordings, voltages were elicited by 100 ms depolarizing steps from a holding potential of −80 mV to test potentials ranging from −80 mV to 50 mV in 10 mV increments. For the latter gene correction experiments, the step length was increased to 200 ms to assay delayed-rectifier currents after more complete decay of transient potassium currents. For retigabine patch applications, resting membrane potential was recorded immediately before and 10 sec after the application of 10 μM retigabine (in each case, membrane potential was an average of values sampled for 20 sec). For all patch experiments, series resistance was monitored by brief −5 pA hyperpolarizing steps during current clamp recordings and by 5 mV hyperpolarizing steps during voltage-clamp recordings. Electrode drift was measured at the end of each recording and was typically 1–2 mV. The extracellular solution was sodium-based and contained 135 mM NaCl, 5 mM KCl, 2 mM $CaCl_2$, 1 mM $MgCl_2$, 10 mM glucose, 10 mM HEPES 10 (pH 7.4). The intracellular solution was potassium based and contained 150 mM KCl, 2 mM $MgCl_2$, 10 mM HEPES, 4 mM MgATP, 0.3 mM NaGTP, 10 mM $Na_2$PhosCr, 1 mM EGTA (pH 7.4). For isolation of delayed-rectifier potassium channels, 300 nM TTX and 100 μM $CdCl_2$ were used to block voltage-gated sodium channels and voltage- and calcium-activated potassium channels, respectively. For isolation of voltage-gated sodium currents, internal KCl was replaced by CsCl to block potassium currents and 100 μM $CdCl_2$ was used to block calcium current.

## Cell Survival and ER Stress Assays

Dissociated neurons (20,000) were plated on poly-D-lysine/laminin coated 8-well chamber slides (BD Biosciences) containing a confluent monolayer of primary cortical mouse glia[21]. For survival analysis, slides were fixed at 3 and 30 days, and cultures were stained for counting. The number of ISL-positive,

TUJ1-positive motor neurons (counter blinded to cell line identity) was normalized to the number on day 3 for each line. Retigabine (1 µM) or vehicle control was added from day 15 onward. Eleven total experiments (control motor neurons) and nine total experiments (ALS motor neurons) were performed from the same four separate differentiations. ER stress experiments were performed as described in Kiskinis et al. (2014). In brief, in two separate independent biological replicates, 300 ng of RNA was used to generate cDNA, of which 2 µl and AmpliTaq Gold Polymerase (Applied Biosystems) were used for PCR amplification. The amounts of spliced and unspliced bands were quantified using Image J. Quantitative RT-PCR was performed in triplicate using the iSCRIPT kit (Bio-Rad) for cDNA synthesis and SYBR green (Bio-Rad) labeling followed by amplification using the iCycler system (Bio-Rad).

## Drugs

Drugs included retigabine (Santa Cruz Biotechnology), bicuculline, strychnine, D-AP5, CNQX, flupirtine, TTX (all from Tocris Bioscience). CsCl and $CdCl_2$ were from Sigma.

## Statistical Analysis

$p < 0.05$ was considered statistically significant. Comparisons were made between control and ALS populations using t tests (two-tailed, unpaired)/ANOVA for continuous data and rank tests for nonparametric data (discrete measurements of number of spikes on ramps and Rheobase). For analysis of MEA firing over time, we used a mixed repeated-measures ANOVA model with fixed effects of cell line and time and random effects of individual replicate.

For effect of retigabine on specific cells, paired tests were used. For effect of retigabine on survival, we fitted a linear regression model with effects of retigabine treatment, cell line, and their interaction. F-tests for difference between ALS and control lines gave $p = 0.0011$, for effect of retigabine $p = 3.8 \times 10^{-4}$, and for effect modification $p = 0.015$. For ALS subjects, the effect of retigabine was an increase in cell count of 25.3% (SD 5.6, $p = 6.4 \times 10-5$). The effect estimate for 39b was 16.9% (SD 12.9, $p = 0.03$) and for RB9d 39.9% (SD 11.3, $p = 0.001$). For control subjects, the effect of retigabine was an increase in cell count of 6.1% (SD 5.1, $p = 0.23$). For multiple genotype comparisons, one-way ANOVA after log transformation to normalize variance and post hoc Tukey tests were used to analyze multiple ALS variants. Error bars represent SEM unless indicated.

# Section 3: Results

## Hyperexcitability of *SOD1*$^{A4V/+}$-Derived Motor Neurons Using MEA Recordings

We performed an initial set of electrophysiological phenotyping experiments using iPSC-derived motor neurons from two control subjects (11a, 18a) and two unrelated familial ALS patients (39b and RB9d) harboring the same aggressive *SOD1*$^{A4V/+}$ mutation. All iPSC lines were generated via three-factor (OCT4, SOX2, KLF4) retroviral reprogramming, had a normal karyotype, and differentiated into motor neurons after robust neutralization based on dual SMAD inhibition[23] and specification through exposure to retinoic acid and induction of sonic hedgehog signaling[18,21] (Figure 1A).

We recorded spontaneous firing of iPSC-derived motor neurons using extracellular MEAs, whereby the action potentials of individual neurons are detected by a grid of 64 extracellular electrodes embedded in each culture well. In four separate experiments, control and *SOD1* ALS iPSC lines were cultured synchronously, differentiated into motor neurons in parallel, and plated in equal numbers on MEAs, which allowed recording of the spontaneous firing in hundreds of control and ALS patient derived neurons per differentiation after culturing for four weeks. We observed significantly more spontaneous action potentials in *SOD1*$^{A4V/+}$ neurons relative to controls ($p < 0.05$, t test; Figures 1B and 1C). Action potentials were sorted by spike morphology and timing to derive clusters corresponding to individual neurons[24] (Figure 2), , and a significantly higher average mean firing rate was observed in the *SOD1*$^{A4V/+}$ neurons ($p < 10^{-15}$, t test; Figures 1D and 1E).

We performed two experiments to confirm that the activity detected by the MEAs resulted intrinsically from motor neurons only. Firstly, to test if differences observed in spontaneous action potential firing resulted from a larger number or a more active population of inhibitory neurons in control cultures, we applied GABAergic and glycinergic transmission blockers. The blockers did not increase action potential firing rates ($p = 0.61$, t test, for bicuculline; $p = 0.24$, t test, for strychnine), suggesting that activity of inhibitory neurons was minimal and that the heightened spontaneous firing in the MEA recordings of ALS-derived motor neurons reflected an intrinsic increase in excitability.

Secondly, we inserted an Hb9::GFP (green fluorescent protein) reporter into the AAVS1 (adeno-associated virus 1) locus for iPSCs 18a and 39b, allowing fluorescence-activated cell sorting (FACS) purification of GFP-positive motor neurons for recording on the arrays. We recorded every four days.

After insertion of the Hb9::GFP reporter into the AAVS1 locus for iPSC lines 18a and 39b, and FACS sorting of neurons, we recorded for four days and observed that 39b Hb9::GFP motor neurons consistently fired more action potentials than 18a Hb9::GFP motor neurons over the entire time course (mixed model ANOVA F-test p = $1x10^{-4}$ for difference between lines; post hoc t tests after Bonferroni correction for multiple comparisons for day 12, p = 0.0055; day 16, p = 0.0030; day 20, p = 0.0057; day 24, p = 0.0029; day 28, p = 0.015; Figure 1F). Thus, the hyperexcitability must be due to motor neurons, because only Hb9-positive motor neurons were plated on the arrays.

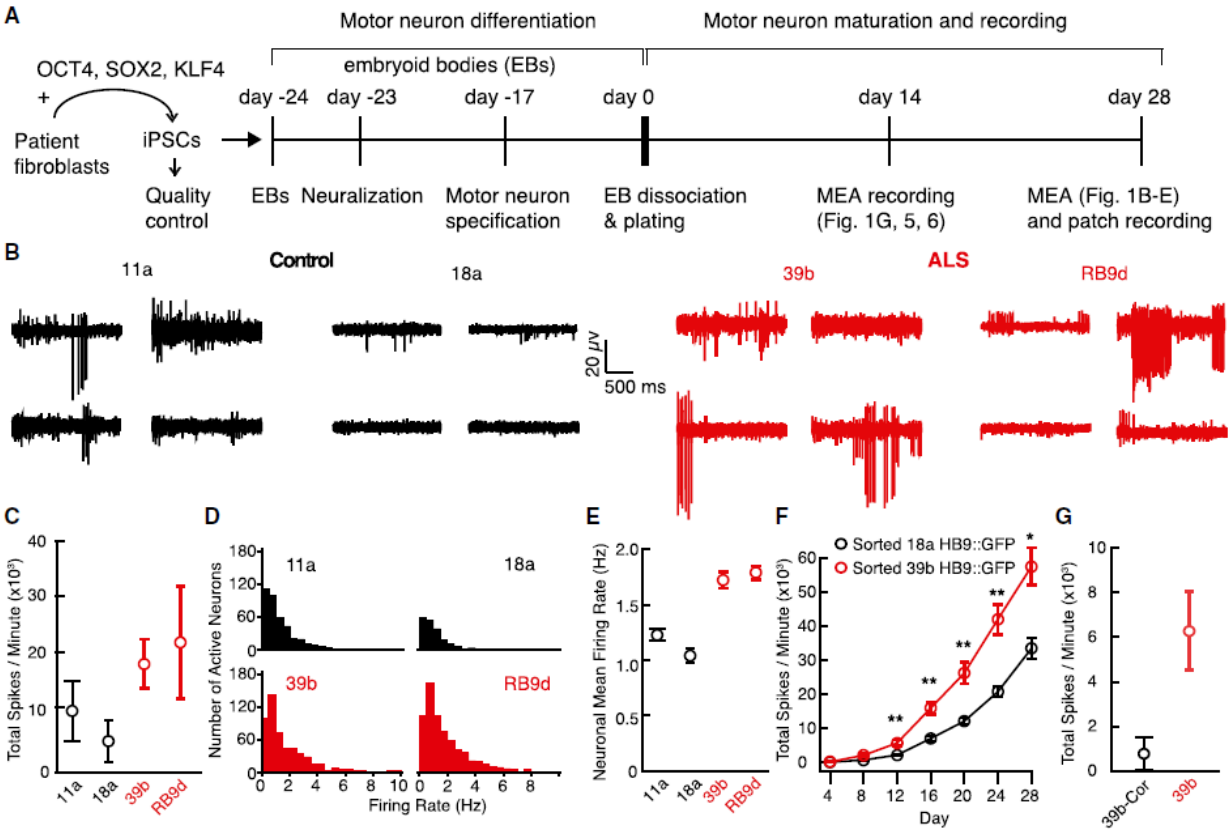


*Figure 1: MEA Recording Reveals Increased Spontaneous Firing in ALS-Derived Neurons Compared to Control-Derived Neurons*

*(A) Schematic of differentiation and recording.*
*(B) Representative recordings from four out of 64 MEA electrodes in control (11a, 18a) and ALS (39b, RB9d)-derived neurons cultured for 28 days on the arrays.*
*(C) Total action potential firing rate during 1 min of recording from MEAs (11a, n = 3; 18a, n = 3; control mean 6,510 ± 3,131 spikes/min; 39b, n = 3; RB9d, n = 3; ALS mean 20,528 ± 5,069 spikes/min; p < 0.05, t test).*
*(D) Mean firing rate histograms of individual neurons from MEAs in (B).*
*(E) Average of mean firing rate for patient-derived neurons (11a, n = 381; 18a, n = 191; control mean 1.17 ± 0.04 Hz; 39b, n = 520; RB9d, n = 662; ALS mean 1.76 ± 0.05 Hz; p < $10^{-15}$, t test).*
*(F) Total action potential firing rate during 1 min recordings from MEAs of FACS-sorted 18a Hb9::GFP and 39b Hb9::GFP motor neurons recorded every 4 days (repeated-measures ANOVA F-test p = 13104 for difference between lines; post hoc t tests with Bonferroni correction for multiple testing indicated as *p < 0.05 and **p < 0.01).*
*(G) Total action potential firing rate during 1min of recording from MEAs cultured for 14 days on the arrays (39b-Cor, n = 4; mean 775 ± 712 spikes/min; 39b, n = 4; 39b mean 6,278 ± 1,758 spikes/min; p = 0.01, t test).*
*Error bars represent SEM.*

## Correction of the *SOD1*$^{A4V/+}$ Mutation Eliminates the Hyperexcitability Phenotype

To test if differences in action potential firing was a direct effect of the *SOD1*$^{A4V/+}$ mutation, we took advantage of a gene-targeted derivative of the 39b iPSC line in which the A4V-encoding mutation had been corrected to a wild-type sequence by homologous recombination, 39b-*SOD1*$^{+/+}$ (abbreviated 39b-Cor) [18], and conducted MEA recordings on it. Because substantial cell death begins in ALS motor neurons after 15 days of neuronal maturation in our culture conditions [18], and because differences in motor neuron firing were detectable at this early time point (Figure 1F), we compared MEA recordings of 39b and isogenic-derived 39b-Cor motor neurons at 14 days, to avoid the possibility that increased firing reflected either neuronal death or select survival of hyperexcitable neurons. Although the baseline spike rate was lower at 14 than 28 days, patient-derived 39b neurons had a higher spontaneous firing rate than neurons in which the *SOD1* mutation was corrected ($p = 0.01$ for total rate, t test; Figure 1G; average mean firing rate 1.30 ± 0.10 Hz for n = 122 39b-Cor and 1.50 ± 0.08 Hz for n = 208 39b; $p < 0.05$, t test). We conclude that the hyperexcitability phenotype reflects the presence of the disease-initiating mutation and precedes progressive motor neuron death.

## Confirmation of ALS Motor Neuron Hyperexcitability and Mechanistic Exploration Using Whole-Cell Patch Clamp

To examine the electrophysiological properties of identified individual motor neurons, we transduced developing neurons with an Hb9::RFP (red fluorescent protein) lentiviral reporter and recorded only from RFP-positive motor neurons[25] using whole-cell patch-clamp (Figure 2A). Both control- and *SOD1* ALS-derived motor neurons were electrically excitable. To quantify the degree of excitability, we assayed the number of action potentials fired in response to a slow ramp depolarization. The number of action potentials fired by ALS motor neurons was significantly greater than control motor neurons ($p < 0.05$, Mann-Whitney U test; Figure 2B, upper panels, Figure 2C, upper panel). Resting membrane potential, action potential threshold (Rheobase), and input resistance did not differ between ALS and control motor neurons, indicating that excitability differences were not due to differences in electrophysiological health or baseline capacity for action potential generation.

When we compared motor neurons derived from 39b-Cor and 39b cell lines in three separate additional parallel experiments, we again observed a marked difference in the number of action potentials elicited

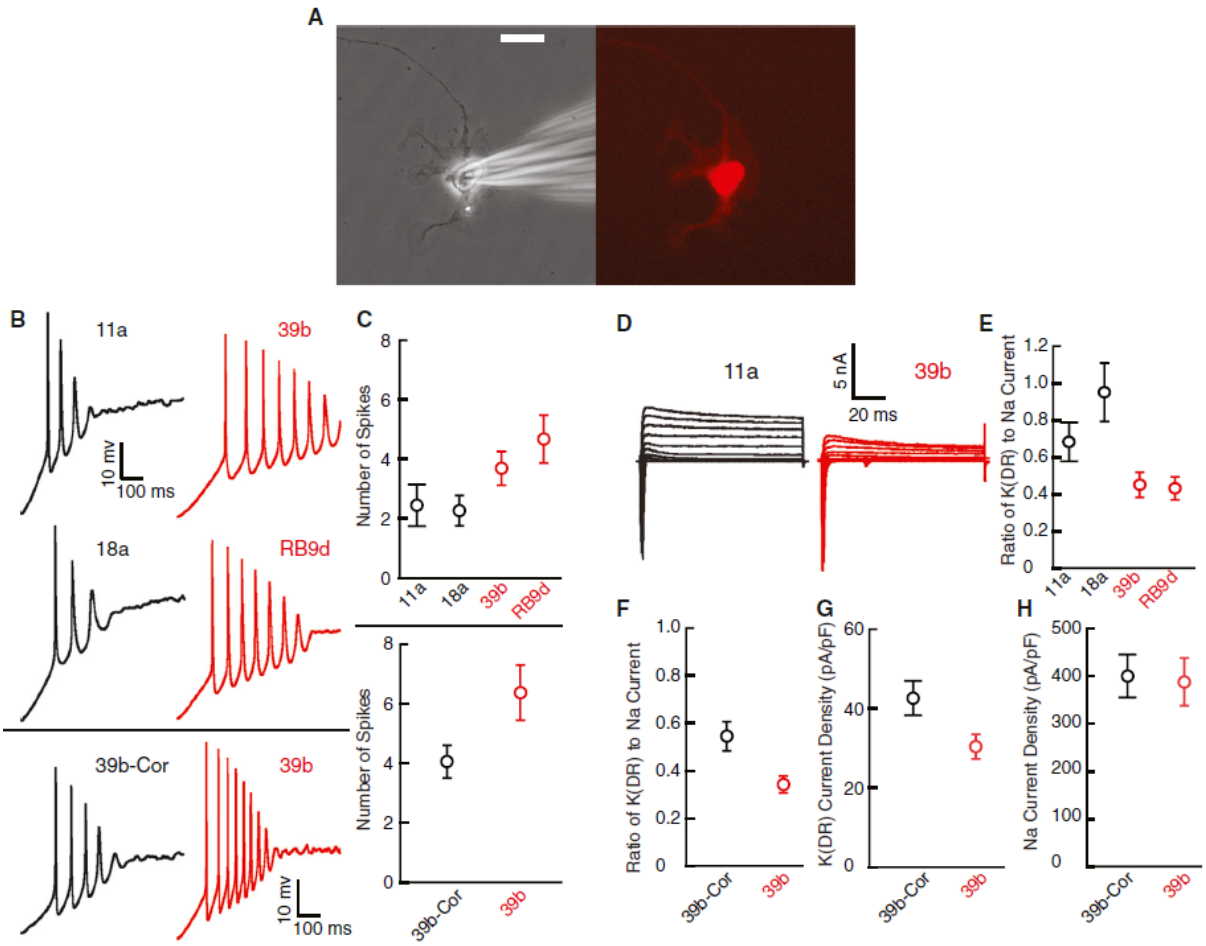


*Figure 2: ALS Patient-Derived Motor Neurons Are Hyperexcitable and Have Reduced Delayed-Rectifier Potassium Currents Compared to Control-Derived Motor Neurons*

*(A) An iPSC-derived motor neuron identified by Hb9::RFP lentiviral transduction (right) and during patch-clamp recording (left) after culture for 28 days. Scale bar, 20 mm.*
*(B) Representative current clamp recordings during ramp depolarization from control and ALS patient-derived motor neurons (upper four panels); sample recordings from separate experiments comparing the isogenic correction of the 39b SOD1$^{A4V/+}$ mutation (39b-Cor) and 39b (lower two panels).*
*(C) Upper panel: average number of action potentials elicited by ramp depolarization from control (11a, n = 12; 18a, n = 11; control mean 2.5 ± 0.4) and ALS (39b, n = 13; RB9d, n = 12; ALS mean 4.2 ± 0.5) motor neurons obtained from four separate differentiations ($p < 0.05$, Mann-Whitney U test). Lower panel: separate experiments showing average number of action potentials during ramp depolarization from 39b-Cor (n = 17; mean 4.1 ± 0.5) and 39b (n = 19; mean 6.4 ± 0.9) motor neurons from three additional differentiations ($p < 0.05$, Mann-Whitney U test).*
*(D) Sample voltage-clamp recordings from control and ALS-derived Hb9::RFP-positive motor neurons cultured for 28 days.*
*(E) Average delayed-rectifier (DR) steady-state potassium current amplitude relative to peak sodium current amplitude in control (11a, n = 12; 18a, n = 11; control mean 0.88 ± 0.087) and ALS (39b, n = 13; RB9d, n = 12; ALS mean 0.44 ± 0.054) patient-derived motor neurons from four differentiations ($p < 0.001$, t test).*
*(F) Experiments from three separate differentiations showing average delayed rectifier steady-state potassium current amplitude relative to peak sodium current amplitude in 39b-Cor (n = 18; mean 0.54 ± 0.061) and 39b (n = 19; mean 0.32 ± 0.036; $p < 0.005$, t test).*
*(G) Direct measurement of delayed-rectifier voltage-gated potassium current isolated by holding at -30 mV, stepping to a test-potential of +40 mV for 2 s and normalizing steady state current amplitude to cell capacitance in 39b-Cor (n = 19; mean 42.6 ± 4.3 pA/pF) and 39b (n = 18; mean 30.3 ± 3.1 pA/pF; $p < 0.05$, t test) derived motor neurons using cells from two additional separate differentiations.*
*(H) Peak sodium current amplitude normalized to cell capacitance in 39b-Cor (n = 16; mean 400.4 ± 44.7 pA/pF) and 39b (n = 15; mean 387.1 ± 50.5 pA/pF; $p = 0.8$, t test) derived motor neurons.*
*Error bars represent SEM.*

during ramp depolarization ($p < 0.05$, Mann-Whitney U test; Figure 2B, lower panels, Figure 2C, lower panel), demonstrating that the A4V mutation was essential for the phenotype. There was variability in the number of action potentials in motor neurons from the same line tested across multiple differentiations, but the increased number of action potentials in ALS motor neurons relative to control motor neurons was always preserved. This result underscores the importance of performing repeated parallel differentiations in which equal numbers of control and ALS motor neurons are analyzed from each differentiation.

In addition to quantifying the electrical excitability of individual neurons, patch-clamp recording enables quantitative investigation of specific currents that determine excitability. To identify electrophysiological mechanisms responsible for differences in excitability, we performed voltage-clamp experiments using Hb9::RFP-positive motor neurons to examine current components. As an index of excitatory and inhibitory voltage-dependent ion channels, we quantified the ratio of outward delayed-rectifier potassium current to inward transient sodium current. In four repeated differentiations of motor neurons from control and *SOD1*$^{A4V/+}$ iPSC lines, we observed that the ratio of delayed-rectifier potassium to transient sodium current was consistently smaller in the *SOD1*$^{A4V/+}$ neurons ($p < 0.001$, t test; Figures 2D and 2E). The difference was driven primarily by the reduced delayed-rectifier potassium channel component, as the difference in steady-state potassium current amplitude normalized to individual cell capacitance between ALS subjects and healthy controls, was significant (control 137.0 ± 14.4 pA/pF, n = 23, versus ALS 94.4 ± 10.7 pA/pF, n = 25; $p < 0.05$, t test), whereas the peak sodium current normalized to capacitance was not (control 190.3 ± 23.0 pA/pF, n = 21, versus ALS 237 ± 21.2 pA/pF, n = 23; $p = 0.2$, t test). Because voltage-gated potassium channels repolarize the membrane potential back to negative values after an action potential, a decrease in such currents likely contributes to increased action potential firing in ALS motor neurons.

Correction of the disease-causing *SOD1*$^{A4V/+}$ mutation also increased the relative steady-state delayed-rectifier potassium current amplitude, showing that this phenotypic difference specifically resulted from the A4V mutation ($p < 0.005$, t test; Figure 2F). We found a marked reduction in delayed-rectifier current magnitude in 39b compared to 39b-Cor motor neurons ($p < 0.05$, t test; Figure 2G) but no difference in sodium current peak amplitudes ($p = 0.8$, t test; Figure 2H). Thus, correction of the deficit in delayed-rectifier potassium current in 39b-Cor motor neurons may enable repolarization of the membrane

potential back to normal hyperpolarized values and reduction of excitability to levels in wild-type motor neurons.

## Retigabine Blocks Motor Neuron Hyperexcitability and Increases in Vitro Survival of *SOD1*$^{A4V/+}$ ALS Motor Neurons

Motor neurons express many types of voltage-activated potassium channels and pharmacological dissection and quantification into distinct components is challenging. Regardless of which currents produce the hyperexcitability in diseased motor neurons, Kv7 (KCNQ) channels are attractive targets for correcting this hyperexcitability because of their activation at subthreshold voltages and subsequent powerful control of excitability[26]. Given this and the reduced delayed-rectifier potassium currents in ALS-derived motor neurons, we hypothesized that retigabine, a specific activator of subthreshold Kv7 currents and clinically approved anticonvulsant[27], might block hyperexcitability in the *SOD1*$^{A4V/+}$ motor neurons. In whole-cell patch clamp, retigabine significantly increased the minimal current step necessary for action potential generation (Rheobase) by 3.6 ± 2.4 pA ($p < 0.05$, Wilcoxon signed rank test; Figure 3A). Retigabine also stopped spontaneous firing of Hb9::RFP-positive motor neurons and hyperpolarized the resting membrane potential by 6.0 ± 2.2 mV ($p = 0.001$, t test; Figure 3B). Because these experiments were performed with blockers of glutamatergic, GABAergic, and glycinergic receptors, retigabine must have a direct effect on motor neuron excitability. We used MEA recordings to determine a dose-response for inhibition of spontaneous firing by retigabine of *SOD1*$^{A4V/+}$ ALS-derived neurons. Retigabine suppressed ALS neuron spontaneous firing with an EC50 of 1.5 mM (Figure 3C), a concentration consistent with its pharmacological activity as an antiepileptic agent and similar to its EC50 for Kv7 channels[28]. In line with this finding, analysis of RNA sequencing (RNA-seq) data from FACS-sorted motor neurons[18] confirm expression of Kv7 channels.

To evaluate the possibility that hyperexcitability is an upstream modulator of motor neuron degeneration in ALS, we tested if retigabine affects the survival of control and *SOD1*$^{A4V/+}$ motor neurons over 30 days in culture. As observed by Kiskinis et al. under basal conditions, the loss of *SOD1*$^{A4V/+}$ motor neurons was greater than *SOD1*$^{+/+}$ control motor neurons[18]. Two weeks of treatment with retigabine (1 mM) increased the number of ALS motor neurons in vitro by 25% ($p < 10^{-4}$, t test; Figure 3D) to levels found in controls.

To investigate how retigabine increases the survival of *SOD1*$^{A4V/+}$ ALS motor neurons, we determined whether it affects pathways suspected to contribute to motor neuron death in ALS[7]. We chose to look at

endoplasmic reticulum (ER) stress because of the demonstration that ER stress pathways are activated in *SOD1*$^{A4V/+}$ ALS compared to *SOD1*$^{+/+}$ motor neurons[18]. After two weeks of treatment with retigabine (1 mM), XBP1 splicing was markedly decreased in retigabine compared to vehicle-treated 39b *SOD1*$^{A4V/+}$ ALS motor neurons. In addition to reduced XBP1 splicing, we observed a decrease in PUMA and increase in EIF2B3 transcript levels, consistent with downregulation of ER stress in response to retigabine treatment.

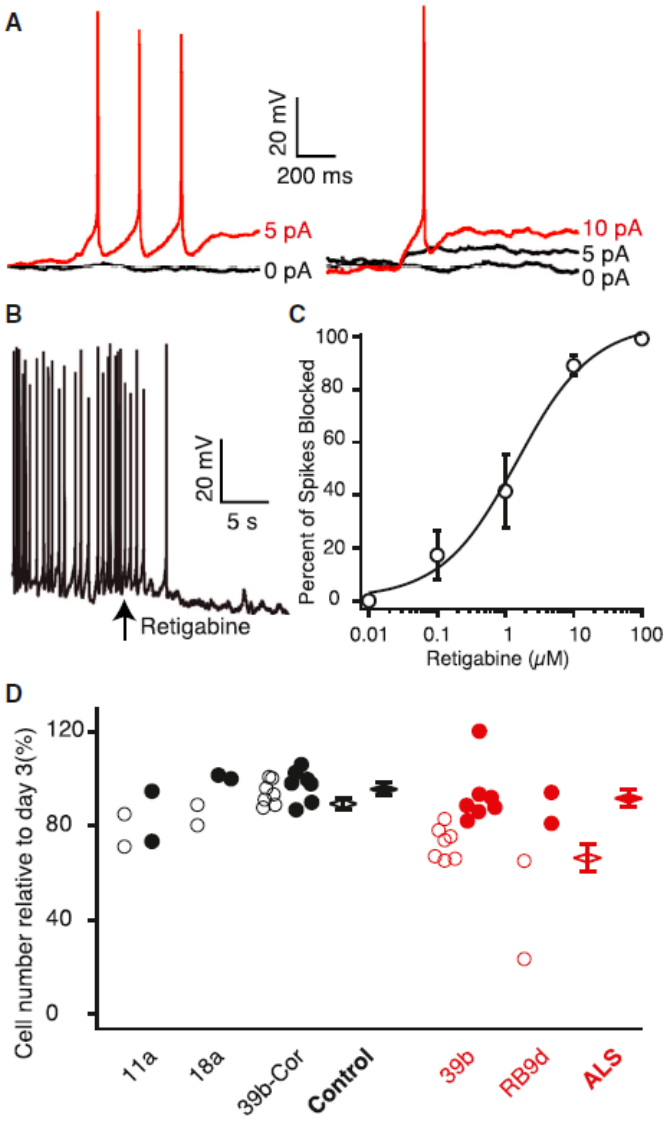


*Figure 3: Retigabine Reduces Motor Neuron Excitability and Increases Survival*

*(A) Rheobase measurements in a 39b Hb9::RFP-positive ALS-derived motor neuron in whole-cell patch clamp before (left) and after (right) the application of 10 mM retigabine (baseline rheobase 4.8 ± 1.5 pA versus post-retigabine rheobase 8.4 ± 2.2 pA; n = 11; p < 0.05, Wilcoxon signed rank test).*
*(B) Representative current clamp recording showing effect of 10 mM retigabine on membrane voltage and spontaneous firing (baseline Vm -60.4 ± 2.9 mV versus post-retigabine Vm -66.3 ± 3.6 mV, n = 11; p = 0.001, t test). In (A) and (B), CNQX (15 mM), D-AP5 (20 mM), bicuculline (25 mM), and strychnine (2.5 mM) were added to the external solution.*
*(C) Dose-response curve for retigabine on suppression of spontaneous action potentials in MEA recording and Hill plot fit of mean data from 39b (n = 4) and RB9d (n = 4) with EC50 1.5 ± 0.8 mM.*
*(D) Effect of vehicle (open circles) and 1mM retigabine (filled circles) treatment from days 14–28 of culture on the survival of Islet-positive, Tuj1-positive motor neurons measured at day 30 (total control n = 11; total ALS n = 9; F-test for effect of retigabine on all cells p = 3.8 3 $10^{-4}$; effect of retigabine in ALS motor neurons, red, 25.3% (SD 5.6; t test p = 6.4 3 $10^{-5}$); effect of retigabine in control motor neurons, black, 6.1% (SD 5.1, p = 0.23). Cell counts are from individual wells for four separate differentiations.*
*Error bars represent SEM.*

## Motor Neuron Hyperexcitability Is Present in Distinct ALS Forms and Is Blocked by Kv7 Activators

In order to investigate whether motor neuron hyperexcitability generalized to additional ALS variants, we performed MEA recordings of motor neurons derived from iPSC lines made from two unrelated familial ALS patients with *C9orf72* hexanucleotide repeat expansion (19f and RB8b)[18], which is responsible for 40 to 50 percent of familial ALS and approximately 10 percent of sporadic cases[7].Motor neurons derived from patients 19f and RB8b, bearing the C9*orf*72 repeat expansion mutation, also showed significant hyperexcitability compared to controls in both total firing rate ($p < 0.05$, t test; Figures 4A and 4B) and average mean neuronal firing rate ($p < 10^{-5}$, t test; Figure 4C).

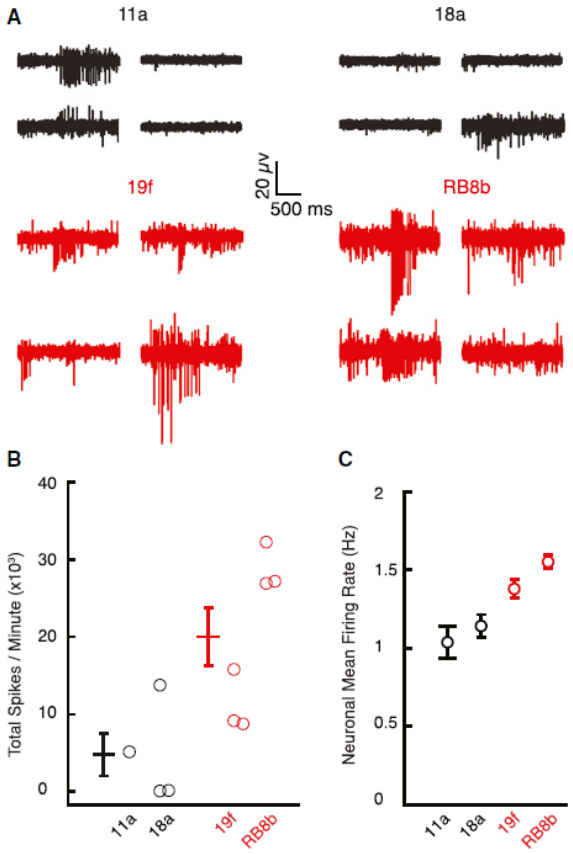


*Figure 4: Hyperexcitability of C9orf72 Repeat Expansion-Derived Motor Neurons*

*(A) Representative recordings from four/64 MEA electrodes recorded from control (11a, 18a) and C9orf72 expansion ALS-derived neurons (19f, RB8b) cultured for 14 days.*
*(B) Total action potential firing rate during 1 min of recording from MEAs (11a, n = 1; 18a, n = 3; control mean 4,752 ± 2,786 spikes/min; 19f, n = 3; RB8b, n = 3; ALS mean 20,022 ± 3,775 spikes/min; $p < 0.05$, t test).*
*(C) Average of mean firing rate for control and C9orf72-derived neurons (11a, n = 82; 18a, n = 203; control mean 1.11 ± 0.06 Hz; 19f, n = 407; RB9d, n = 929; ALS mean 1.50 ± 0.04; $p < 10^{-5}$, t test).*
*Error bars represent SEM.*

We reasoned that comparing neuronal firing properties of a large group of ALS patient and control-derived motor neurons would help evaluate the robustness of the motor neuron hyperexcitability and, together with the A4V gene correction experiments, eliminate artifacts due to cell line variation. *SOD1*-derived motor neurons (four lines from four unrelated subjects harboring three different mutations), C9orf72-derived motor neurons (two lines from two unrelated subjects), FUS-derived motor neurons

(two lines from two unrelated subjects harboring two different mutations) were all hyperexcitable relative to motor neurons derived from six iPSC lines made from five individual healthy controls (ANOVA, $p < 10^{-7}$; Tukey's post hoc tests for control versus *SOD1* $p < 0.01$, control versus C9orf72 $p < 0.01$, control versus FUS $p < 0.05$; Figure 5A). Furthermore, spontaneous action potential firing in the ALS variant-derived motor neurons was uniformly blocked by retigabine (Figure 5B). Consistent with an on-target effect of retigabine, we found that a chemically distinct but less potent Kv7 current enhancer, flupirtine[26], also blocked spontaneous motor neuron firing (Figure 5C). These results demonstrate the broad relevance of motor neuron hyperexcitability for familial ALS and its sensitivity to Kv7 agonists across iPSC lines, patients and genotypic etiologies.

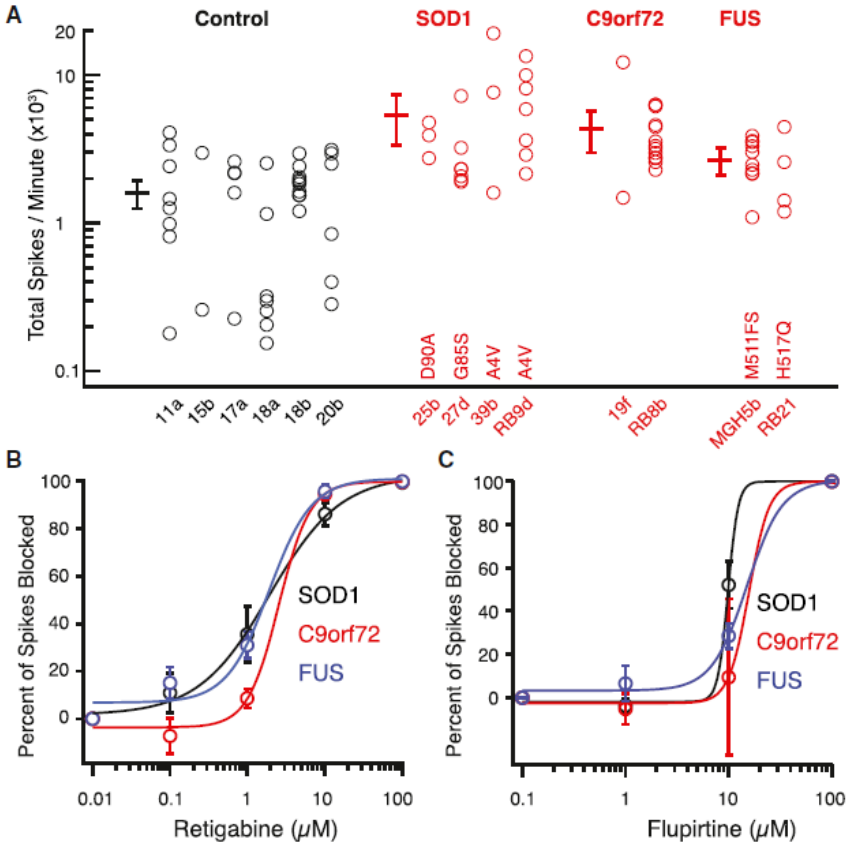


*Figure 5: Motor Neuron Hyperexcitability and Block by Retigabine Are Broad Properties of ALS Variants*

*(A) Multielectrode array recordings of motor neurons derived from control (11a, n = 8; 15b, n = 2; 17a, n = 5; 18a, n = 7; 18b, n = 10; 20b, n = 6), SOD1 (25b, D90A, n = 3; 27d, G85S, n = 7; 39b, A4V, n = 3; RB9d, A4V, n = 7), C9orf72 expansion (19f, n = 2; RB8B, n = 13) and FUS (MGH5b, frameshift mutation at residue 511, n = 10; RB21, H517Q, n = 4) subjects cultured for 14 days. ANOVA, $p < 10^{-7}$; Tukey's post hoc tests for control versus SOD1 $p < 0.01$, control versus C9orf72 $p < 0.01$, control versus FUS $p < 0.05$. For subject 18, motor neurons from two different iPSC lines were recorded. Error bars are 95% confidence interval.*
*(B) Dose-response curve for retigabine on suppression of spontaneous action potentials in MEA recording and Hill plot fit of mean data from SOD1 (n = 10; $EC_{50}$ 1.9 ± 0.5 mM), C9orf72 (n = 9; $EC_{50}$ 2.6 ± 0.8 mM) and FUS (n = 4; $EC_{50}$ 1.9 ± 1.1 mM).*
*(C) Dose-response curve for flupirtine on suppression of spontaneous action potentials in MEA recording and Hill plot fit of mean data from SOD1 (n = 5; $EC_{50}$ 9.8 mM), C9orf72 (n = 4; $EC_{50}$ 19.4 mM) and FUS (n = 2; $EC_{50}$ 15 mM).*
*Error bars for (B) and (C) represent SEM.*

We ultimately analyzed four lines from four unrelated subjects (25b, 27d, 39b, RB8da) harboring three different mutations of the *SOD1* gene, two lines from two unrelated subjects (19f and RB8b) bearing the C9*orf*72 repeat expansion mutation, and two lines from two unrelated subjects (MGH5b, RB21) bearing two different mutations.

## Section 4: Discussion

Neurons derived from patient iPSCs can be used to investigate physiologic changes in specific neural subtypes relevant to neurodegeneration and reveal important disease mechanisms and candidate therapeutics. We found consistent hyperexcitability in motor neurons from a broad group of familial ALS patients, whose disease-causing mutations collectively span the majority of familial ALS cases. Differential excitability of particular motor neurons has been proposed to explain the selective vulnerability of specific motor neuron pools in ALS, and our data provide a possible mechanistic basis for this hypothesis[29,30].

Motor neuron hyperexcitability may contribute, therefore, to motor neuron death, although connections between hyperexcitability and motor neuron death in other ALS variants will now require further investigation. Our results are consistent with multiple studies exploring excitotoxicity[6,31] but, potentially, not with two recent studies. One postulated that increased excitability in the h*SOD1*(G93A) mouse model may be a compensatory mechanism[32]. However, systemically administered glutamatergic and cholinergic modulators may affect multiple neuronal types, making it difficult to assess how the findings relate to motor neuron excitability, which was not measured. A second study found decreased numbers of elicited spikes in iPSC-derived motor neurons from ALS patients with C9*orf*72 repeat expansion compared to controls[33]. The differences in spike count here may reflect the longer differentiation time (66–79 days), differences in surviving neuronal populations or alterations in resting membrane potential in C9*orf*72 compared to control neurons. For example, the more depolarized resting potential in C9*orf*72 expansion-derived neurons could result in greater sodium channel inactivation and reduced capacity for generation of multiple action potentials; indeed, depolarization induced action potential blockade may be a late phase of progressive hyperexcitability. Mouse h*SOD1*(G93A) motor neurons show hyperexcitability even at an embryonic age[13,34,35], and neurophysiological studies reveal increased excitability in C9*orf*72 repeat expansion subjects[36] in addition to other familial and sporadic ALS cases[12,14,37,38].

Previously, attention has been focused on persistent sodium currents as a mechanism of motor neuron hyperexcitability[14,39], and riluzole, the only approved drug for ALS, blocks this current[40]. Our findings suggest an additional important role of voltage-activated potassium channels.

Channel compartmentalization may differ between in vivo and cultured-neuron systems; however, a recent immunohistochemical study of human spinal cords found decreased protein levels of a delayed-rectifier potassium channel selectively in the ventral roots of sporadic ALS but not control subjects[41]. Mutations in voltage-gated potassium channels cause other neurodegenerative diseases[42], and oxidation of potassium channels (with consequent modulation of voltage-dependence and kinetics of channel gating) has been suggested as a broad mechanism of aging and neurodegeneration[43]. DPP6, which is involved with in-trafficking Kv4 voltage-gated potassium channels in CA1 hippocampal neurons, is linked to ALS[44,45]. Hypermethylation and downregulation of potassium channel genes were observed in epigenetic analyses of postmortem ALS patient spinal cords[46].

Both enhanced persistent sodium and reduced potassium currents could converge to produce hyperexcitability, and both may offer complementary pharmacological targets to control it.

Although our study evaluated hyperexcitability as an innate or autonomous property of motor neurons, differences in excitability may also reflect interactions between motor neurons and glia or Schwann cells[31]. Hyperexcitability has also been observed in motor neurons from a mouse model of spinal muscular atrophy[47], and there is evidence for both cell autonomous[48] and nonautonomous[49] modulation of excitability.

Interestingly, spinal muscular atrophy has also been linked to DPP6, raising the possibility of potassium channel contributions[50].

The pathways connecting disease-causing mutations and decreased potassium channel function, as well as hyperexcitability and motor neuron death continue to require further clarification. Calcium overload through voltage-gated calcium channels[51] and activation of ER stress[30] are possibilities. The finding that decreasing motor neuron activity reduces ER stress suggests that hyperexcitability may be upstream of the unfolded protein response, explaining at least partially, how hyperexcitability may contribute to motor neuron death in ALS. Because ER stress modifiers increase motor neuron activity, a vicious cycle may result in ALS from reciprocal positive feedback between hyperactivity and ER stress[18].

Despite the asymptomatic early decades typical of ALS patients, we observed a disease-specific phenotype in iPSC-derived neurons cultured for only weeks. That this property manifests so quickly in culture may reflect the absence of supporting cells and the inhibitory circuitry normally present in vivo. Identification of a screenable electrophysiological phenotype that contributes to motor neuron death

and manifests quickly could facilitate investigation of ALS pathophysiology and identification or validation of therapeutics for individual patients. Furthermore, the phenotype may offer a personalized medicine approach to treatment, using response of stem cell-derived neurons as a guide for individual patient treatment selection; this strategy will require motor neurons derived from large cohorts of patients for validation. Studies of motor neuron excitability can now be expanded to determine whether all forms of ALS converge onto a single mechanistic pathway. More generally, our study illustrates the potential for using iPSCs differentiated into specific disease-relevant cell types to identify disease phenotypes, novel biomarkers, and potential treatments.

# References


1. Kiernan MC, Vucic S, Cheah BC, Turner MR, Eisen A, Hardiman O, Burrell JR, Zoing MC. Amyotrophic lateral sclerosis. *The Lancet*. Elsevier Ltd; 2011;377(9769):942–55.

2. Pasinelli P, Brown RH. Molecular biology of amyotrophic lateral sclerosis: insights from genetics. *Nature reviews Neuroscience*. 2006;7(September):710–23.

3. Rowland LP. How Amyotrophic Lateral Sclerosis Got Its Name. *Archives of Neurology*. 2001;58:512–5.

4. Worms PM. The epidemiology of motor neuron diseases: a review of recent studies. *Journal of the neurological sciences*. 2001;191:3–9.

5. Logroscino G, Traynor BJ, Hardiman O, Chiò A, Mitchell D, Swingler RJ, Millul A, Benn E, Beghi E. Incidence of amyotrophic lateral sclerosis in Europe. *Journal of neurology, neurosurgery, and psychiatry*. 2010;81:385–90.

6. Cleveland DW, Rothstein JD. From Charcot to Lou Gehrig: deciphering selective motor neuron death in ALS. *Nature reviews Neuroscience*. 2001;2(November):806–19.

7. Robberecht W, Philips T. The changing scene of amyotrophic lateral sclerosis. *Nature reviews Neuroscience*. Nature Publishing Group; 2013;14(March):248–64.

8. Rohrer JD, Isaacs AM, Mizlienska S, Mead S, Lashley T, Wray S, Sidle K, Fratta P, Orrell RW, Hardy J, Holton J, Revesz T, Rossor MN, Warren JD. C9orf72 expansions in frontotemporal dementia and amyotrophic lateral sclerosis. *The Lancet Neurology*. 2015;291–301.

9. Bostock H, Sharief MK, Reid G, Murray NM. Axonal ion channel dysfunction in amyotrophic lateral sclerosis. *Brain : a journal of neurology*. 1995;118 ( Pt 1:217–25.

10. Kanai K, Kuwabara S, Misawa S, Tamura N, Ogawara K, Nakata M, Sawai S, Hattori T, Bostock H. Altered axonal excitability properties in amyotrophic lateral sclerosis : impaired potassium channel function related to disease stage. 2006;953–62.

11. Nakata M, Kuwabara S, Kanai K, Misawa S, Tamura N, Sawai S, Hattori T, Bostock H. Distal excitability changes in motor axons in amyotrophic lateral sclerosis. *Clinical Neurophysiology*. 2006;117:1444–8.

12. Vucic S, Kiernan MC. Axonal excitability properties in amyotrophic lateral sclerosis. *Clinical Neurophysiology*. 2006;117:1458–66.

13. Van Zundert B, Peuscher MH, Hynynen M, Chen A, Neve RL, Brown RH, Constantine-Paton M, Bellingham MC. Neonatal neuronal circuitry shows hyperexcitable disturbance in a mouse model of the adult-onset neurodegenerative disease amyotrophic lateral sclerosis. *The Journal of neuroscience : the official journal of the Society for Neuroscience*. 2008;28(43):10864–74.

14. Vucic S, Kiernan MC. Upregulation of persistent sodium conductances in familial ALS. *Journal of neurology, neurosurgery, and psychiatry*. 2010;81:222–7.

15. Takahashi K, Tanabe K, Ohnuki M, Narita M, Ichisaka T, Tomoda K, Yamanaka S. Induction of Pluripotent Stem Cells from Adult Human Fibroblasts by Defined Factors. *Cell*. 2007;131:861–72.

16. Dimos JT, Rodolfa KT, Niakan KK, Weisenthal LM, Mitsumoto H, Chung W, Croft GF, Saphier G, Leibel R, Goland R, Wichterle H, Henderson CE, Eggan K. Induced pluripotent stem cells generated from patients with ALS can be differentiated into motor neurons. *Science (New York, NY)*. 2008;321(August):1218–21.

17. Sandoe J, Eggan K. Opportunities and challenges of pluripotent stem cell neurodegenerative disease models. *Nature Neuroscience*. Nature Publishing Group; 2013;16(7):780–9.

18. Kiskinis E, Sandoe J, Williams L a., Boulting GL, Moccia R, Wainger BJ, Han S, Peng T, Thams S, Mikkilineni S, Mellin C, Merkle FT, Davis-Dusenbery BN, Ziller M, Oakley D, Ichida J, Di Costanzo S, Atwater N, Maeder ML, Goodwin MJ, Nemesh J, Handsaker RE, Paull D, Noggle S, McCarroll S a., Joung JK, Woolf CJ, Brown RH, Eggan K. Pathways disrupted in human ALS motor neurons identified through genetic correction of mutant SOD1. *Cell Stem Cell*. Elsevier Inc.; 2014;14(6):781–95.

19. Wainger BJ, Kiskinis E, Mellin C, Wiskow O, Han SSW, Sandoe J, Perez NP, Williams L a., Lee S, Boulting G, Berry JD, Brown RH, Cudkowicz ME, Bean BP, Eggan K, Woolf CJ. Intrinsic membrane hyperexcitability of amyotrophic lateral sclerosis patient-derived motor neurons. *Cell Reports*. 2014;7(1):1–11.

20. Bock C, Kiskinis E, Verstappen G, Gu H, Boulting G, Smith ZD, Ziller M, Croft GF, Amoroso MW, Oakley DH, Gnirke A, Eggan K, Meissner A. Reference maps of human es and ips cell variation enable high-throughput characterization of pluripotent cell lines. *Cell*. 2011;144:439–52.

21. Boulting GL, Kiskinis E, Croft GF, Amoroso MW, Oakley DH, Wainger BJ, Williams DJ, Kahler DJ, Yamaki M, Davidow L, Rodolfa CT, Dimos JT, Mikkilineni S, MacDermott a B, Woolf CJ, Henderson CE, Wichterle H, Eggan K. A functionally characterized test set of human induced pluripotent stem cells. *Nat Biotechnol*. 2011;29(3):279–86.

22. Boehler MD, Wheeler BC, Brewer GJ. Added astroglia promote greater synapse density and higher activity in neuronal networks. Neuron Glia Biology. 2007.

23. Chambers SM, Fasano C a, Papapetrou EP, Tomishima M, Sadelain M, Studer L. Highly efficient neural conversion of human ES and iPS cells by dual inhibition of SMAD signaling. *Nature biotechnology*. 2009;27(3):275–80.

24. Cohen MR, Kohn A. Measuring and interpreting neuronal correlations. *Nature neuroscience*. 2011 Jul;14(7):811–9.

25. Marchetto MCN, Muotri AR, Mu Y, Smith AM, Cezar GG, Gage FH. Non-cell-autonomous effect of human SOD1 G37R astrocytes on motor neurons derived from human embryonic stem cells. *Cell stem cell*. Elsevier Inc.; 2008;3(6):649–57.

26. Brown D a., Passmore GM. Neural KCNQ (Kv7) channels. *British Journal of Pharmacology*. 2009;156(November 2008):1185–95.

27. Porter RJ, Partiot a., Sachdeo R, Nohria V, Alves WM. Randomized, multicenter, dose-ranging trial of retigabine for partial-onset seizures. *Neurology*. 2007;68:1197–204.

28. Wickenden a D, Yu W, Zou a, Jegla T, Wagoner PK. Retigabine, a novel anti-convulsant, enhances activation of KCNQ2/Q3 potassium channels. *Molecular pharmacology*. 2000;58(3):591–600.

29. Jong SB, Sawai S, Misawa S, Kanai K, Isose S, Kuwabara S. Differences in excitability properties of FDI and ADM motor axons. *Muscle and Nerve*. 2009;39(March):350–4.

30. Saxena S, Caroni P. Selective Neuronal Vulnerability in Neurodegenerative Diseases: From Stressor Thresholds to Degeneration. *Neuron*. Elsevier Inc.; 2011;71(1):35–48.

31. Fritz E, Izaurieta P, Weiss A, Mir FR, Rojas P, Gonzalez D, Rojas F, Brown RH, Madrid R, van Zundert B. Mutant SOD1-expressing astrocytes release toxic factors that trigger motoneuron death by inducing hyperexcitability. *Journal of neurophysiology*. 2013;109:2803–14.

32. Saxena S, Roselli F, Singh K, Leptien K, Julien JP, Gros-Louis F, Caroni P. Neuroprotection through Excitability and mTOR Required in ALS Motoneurons to Delay Disease and Extend Survival. *Neuron*. Elsevier Inc.; 2013;80(1):80–96.

33. Sareen D, O'Rourke JG, Meera P, Muhammad a KMG, Grant S, Simpkinson M, Bell S, Carmona S, Ornelas L, Sahabian A, Gendron T, Petrucelli L, Baughn M, Ravits J, Harms MB, Rigo F, Bennett CF, Otis TS, Svendsen CN, Baloh RH. Targeting RNA foci in iPSC-derived motor neurons from ALS patients with a C9ORF72 repeat expansion. *Science translational medicine*. 2013;5(208):208ra149.

34. Kuo JJ, Schonewille M, Siddique T, Schults AN a, Fu R, Bär PR, Anelli R, Heckman CJ, Kroese AB a. Hyperexcitability of cultured spinal motoneurons from presymptomatic ALS mice. *Journal of neurophysiology*. 2004;91(October 2003):571–5.

35. Pieri M. Altered excitability of motor neurons in a transgenic mouse model of familial amyotrophic lateral sclerosis. *Neuroscience Letters*. 2003;351:153–6.

36. Williams KL, Fifita J a, Vucic S, Durnall JC, Kiernan MC, Blair IP, Nicholson G a. Pathophysiological insights into ALS with C9ORF72 expansions. *Journal of Neurology, Neurosurgery & Psychiatry*. 2013;84:931–5.

37. Blair IP, Williams KL, Warraich ST, Durnall JC, Thoeng AD, Manavis J, Blumbergs PC, Vucic S, Kiernan MC, Nicholson G a. FUS mutations in amyotrophic lateral sclerosis: clinical, pathological,

neurophysiological and genetic analysis. *Journal of neurology, neurosurgery, and psychiatry*. 2010;81:639–45.

38. Mills KR, Nithi K a. Corticomotor threshold is reduced in early sporadic amyotrophic lateral sclerosis. *Muscle and Nerve*. 1997;20(September):1137–41.

39. Kuo JJ, Siddique T, Fu R, Heckman CJ. Increased persistent Na(+) current and its effect on excitability in motoneurones cultured from mutant SOD1 mice. *The Journal of physiology*. 2005;563:843–54.

40. Urbani a., Belluzzi O. Riluzole inhibits the persistent sodium current in mammalian CNS neurons. *European Journal of Neuroscience*. 2000;12:3567–74.

41. Shibuya K, Misawa S, Arai K, Nakata M, Kanai K, Yoshiyama Y, Ito K, Isose S, Noto YI, Nasu S, Sekiguchi Y, Fujimaki Y, Ohmori S, Kitamura H, Sato Y, Kuwabara S. Markedly reduced axonal potassium channel expression in human sporadic amyotrophic lateral sclerosis: An immunohistochemical study. *Experimental Neurology*. Elsevier Inc.; 2011;232(2):149–53.

42. Waters MF, Minassian NA, Stevanin G, Figueroa KP, Bannister JPA, Nolte D, Mock AF, Evidente VGH, Fee DB, Mu U, Brice A, Papazian DM, Pulst SM. Mutations in voltage-gated potassium channel KCNC3 cause degenerative and developmental central nervous system phenotypes. 2006;38(4):447–51.

43. Sesti F, Liu S, Cai SQ. Oxidation of potassium channels by ROS: a general mechanism of aging and neurodegeneration? *Trends in Cell Biology*. 2010;20(October):45–51.

44. Sun W, Maffie JK, Lin L, Petralia RS, Rudy B, Hoffman DA. DPP6 Establishes the A-Type K+ Current Gradient Critical for the Regulation of Dendritic Excitability in CA1 Hippocampal Neurons. *Neuron*. 2011;71:1102–15.

45. Van Es M a, van Vught PWJ, Blauw HM, Franke L, Saris CGJ, Van den Bosch L, de Jong SW, de Jong V, Baas F, van't Slot R, Lemmens R, Schelhaas HJ, Birve A, Sleegers K, Van Broeckhoven C, Schymick JC, Traynor BJ, Wokke JHJ, Wijmenga C, Robberecht W, Andersen PM, Veldink JH, Ophoff R a, van den Berg LH. Genetic variation in DPP6 is associated with susceptibility to amyotrophic lateral sclerosis. *Nature genetics*. 2008;40(1):29–31.

46. Figueroa-Romero C, Hur J, Bender DE, Delaney CE, Cataldo MD, Smith AL, Yung R, Ruden DM, Callaghan BC, Feldman EL. Identification of Epigenetically Altered Genes in Sporadic Amyotrophic Lateral Sclerosis. *PLoS ONE*. 2012;7(12).

47. Mentis GZ, Blivis D, Liu W, Drobac E, Crowder ME, Kong L, Alvarez FJ, Sumner CJ, O'Donovan MJ, Melissa E, Kong L, Alvarez FJ, Sumner CJ, Michael J, Donovan O. Early Functional Impairment of Sensory-Motor Connectivity in a Mouse Model of Spinal Muscular Atrophy. *Neuron*. 2011;69(3):453–67.

48. Gogliotti RG, Quinlan K a., Barlow CB, Heier CR, Heckman CJ, DiDonato CJ. Motor Neuron Rescue in Spinal Muscular Atrophy Mice Demonstrates That Sensory-Motor Defects Are a Consequence, Not a Cause, of Motor Neuron Dysfunction. *Journal of Neuroscience*. 2012;32(11):3818–29.

49. Imlach WL, Beck ES, Choi BJ, Lotti F, Pellizzoni L, McCabe BD. SMN is required for sensory-motor circuit function in drosophila. *Cell*. 2012;151(2):427–39.

50. Van Es MA, van Vught PWJ, van Kempen G, Blauw HM, Veldink JH, van den Berg LH. Dpp6 is associated with susceptibility to progressive spinal muscular atrophy. *Neurology*. 2009;72:1184–5.

51. Chan CS, Guzman JN, Ilijic E, Mercer JN, Rick C, Tkatch T, Meredith GE, Surmeier DJ. "Rejuvenation" protects neurons in mouse models of Parkinson's disease. *Nature*. 2007;447(June):1081–6.

# Tables and Figures